Lab on a Chip

Accepted Manuscript

ROYAL SOCIETY OF CHEMISTRY

www.rsc.org/loc

Lab on a Chip

RSCPublishing

ARTICLE

A lung-on-chip array with an integrated bio-inspired respiration mechanism

Cite this: DOI: 10.1039/x0xx00000x

Andreas O. Stucki,‡[ab] Janick D. Stucki,‡[ab] Sean R. R. Hall,[de] Marcel Felder,[ab] Yves Mermoud,[a] Ralph A. Schmid,[de] Thomas Geiser,[ce] Olivier T. Guenat§[acd]

Received 00th xxx,
Accepted 00th xxx

DOI: 10.1039/x0xx00000x

www.rsc.org/

We report about a lung-on-chip array that mimics the pulmonary parenchymal environment, including the thin, alveolar barrier and the three-dimensional cyclic strain induced by the breathing movements. A micro-diaphragm used to stretch the alveolar barrier is inspired by the in-vivo diaphragm, the main muscle responsible for inspiration. The design of this device aims not only at best reproducing the in-vivo conditions found in the lung parenchyma, but also at making its handling easy and robust. An innovative concept, based on the reversible bonding of the device, is presented that enables to accurately control the concentration of cells cultured on the membrane by easily accessing both sides of the membranes. The functionality of the alveolar barrier could be restored by co-culturing epithelial and endothelial cells that formed tight monolayers on each side of a thin, porous and stretchable membrane. We showed that cyclic stretch significantly affects the permeability properties of epithelial cell layers. Furthermore, we could also demonstrate that the strain influences the metabolic activity and the cytokine secretion of primary human pulmonary alveolar epithelial cells obtained from patients. These results demonstrate the potential of this device and confirm the importance of the mechanical strain induced by the breathing in pulmonary research.

Introduction

The pharmaceutical sector is currently experiencing a serious efficiency crisis that forces all the actors in this field to rethink the way research and development can be performed more efficiently.[1] One of the key issues that urgently needs to be addressed is the lack of efficient and reproducible drug discovery models able to predict the toxicity and the efficiency of compounds in humans prior to launch expensive clinical trials. Animal models used in the preclinical phase often poorly predict the toxicological responses in humans[2] and standard in-vitro models fail to reproduce the complexity of the biophysical and cellular microenvironment found in-vivo. Recent progresses in microtechnologies have enabled the emergence of novel in-vitro models that better reproduce the physiological resemblance and relevance.[3] These models called "organs-on-chip" are widely seen as being able to better predict the human response and simultaneously to importantly reduce the ethically controversial animal testing.

Lung-on-chips aiming at mimicking the complex microenvironment of the lung alveoli have only recently been reported. In sharp contrast to standard in-vitro models, such systems allow to reproduce the cyclic mechanical stress induced by the respiratory movements. Takayama and colleagues investigated the mechanical stress induced by liquid plug propagation in small flexible airway models and suggested that the possibility of induced injuries on lining cells along the airways in emphysema is higher due to the larger wall stresses.[4] His group further studied the combined effect of mechanical and surface-tension stresses that typically occur in ventilator induced lung injury.[5] Using this device, they demonstrated cellular-level lung injury under flow conditions that caused symptoms characteristic of a wide range of pulmonary diseases.[6] More recently, Ingber and colleagues reported about a lung alveolus model that further reproduces the in-vivo situation by mimicking the thin alveolar barrier being cyclically stretched.[7] The barrier made of a thin, porous and stretchable poly-dimethylsiloxane (PDMS) membrane on which epithelial and endothelial cells are cultured, is sandwiched between two microfluidic structures creating two superposed microchannels. The actuation

[a]*ARTORG Center for Biomedical Engineering Research, Lung Regeneration Technologies, University of Berne, Switzerland.*
[b]*Graduate School for Cellular and Biomedical Sciences, University of Berne, Switzerland.*
[c]*Division of Pulmonary Medicine, University Hospital of Berne, Switzerland.*
[d]*Division of Thoracic Surgery, University Hospital of Berne, Switzerland.*
[e]*Department of Clinical Research, University of Berne, Switzerland.*
‡*These authors contributed equally to this work.*
§*Corresponding author.*
† *Electronic Supplementary Information (ESI) available: Movie of real-time stretching of primary cells, chip handling, strain characterization and immunofluorescence images.*

mechanism resulting in the cyclic strain of the PDMS membrane is performed by varying a negative pressure in two channels located on each side of the superposed microchannels and separated from it by thin walls. This actuation principle presents the drawback that the strain applied to the thin, porous membrane strongly depends on the viscoelastic properties of the stretched material (here PDMS) and on the dimensions, in particular the thickness, of the thin PDMS walls. Consequently, the negative pressure applied in the adjacent channels needs to be precisely controlled. In addition, the typical, confined microfluidic setting used, does not allow to precisely control the concentration of cells seeded on the membrane.

Furthermore, the in-vivo relevance of almost all in-vitro human lung alveolar models is limited by the use of lung epithelial cell line or primary lung cells from rats. Unfortunately, the most used lung epithelial cells, A549, is a lung adenocarcinoma cell line that poorly mimics the phenotype of original pulmonary alveolar epithelial cells. On the other hand, primary lung cells from rats suffer from interspecies difference and are thus inadequate to recreate a human air-blood barrier.

We report here about a novel lung-on-chip that does not suffer from these limitations. It mimics the lung alveolar barrier in an unprecedented way, using primary human pulmonary alveolar epithelial cells obtained from patients undergoing partial lung resection. The lung alveolar barrier can be exposed to a 3D cyclic mechanical strain, using a novel bioinspired actuation mechanism. Experiments performed with those cells and lung bronchial epithelial cells reveal the significance of the mechanical strain on those cells. This robust and easy to use lung-on-chip is intended to be a tool for the drug discovery development as well as for the toxicology fields in research and industry.

Materials and Methods

Fabrication of the lung-on-chip

The lung-on-chip consists of a fluidic and a pneumatic part (Fig. 1C). The fluidic part comprises two PDMS plates between which a thin, porous and flexible PDMS membrane is sandwiched and bonded. The top plate contains a 3mm in diameter access hole to the apical side of the membrane, and a 1mm in diameter hole to access the overflow chamber. The bottom plate is structured with a cell culture medium reservoir. The pneumatic part is made of a 40µm thin PDMS layer bonded with the actuation plate in which pneumatic channels are structured. The fluidic and pneumatic parts are made by soft lithography.[8] Briefly, PDMS base and curing agents (Sylgard 184, Dow Corning) are mixed well (10:1 w/w ratio), degased in a vacuum desiccator and casted in hard plastic molds made directly from aluminum molds structured by standard machining (ki-Mech GmbH). The PDMS pre-polymer is cured at 60°C for at least 24 hours. The porous and flexible membrane is fabricated by a microstructuring-lamination process. The PDMS pre-polymer is sandwiched between a silicon mold containing an array of micropillars structured by DRIE and a 75µm thin PE sheet (DuPont Teijin Films, Melinex® 411). The micropillars have different heights ranging from 3.5µm up to 10µm and different diameters (3µm or 8µm), in function of the characteristic of the membrane. The silicon mold and the plastic sheet are then clamped together with the PDMS pre-polymer sandwiched in between and cured at 60°C for at least 24 hours. The thickness of the produced membrane corresponds to the height of the micropillars, which have pores of 3 or 8µm in diameter (Fig. 2A). After curing, the membrane was released from the mold and irreversibly bonded by O2 plasma (Harrick Plasma) onto the bottom plate. The top plate was then reversibly bonded to the bottom plate. The thin PDMS layer in which the micro-diaphragm is included is fabricated by spinning PDMS pre-polymer onto a PE sheet attached to a silicon wafer at 1700rpm for 60 seconds. After spinning, the membrane was allowed to cure for 24 hours at 60°C and was then irreversibly bonded by O2 plasma on the actuation plate.

Cell culture protocols

Bronchial epithelial 16HBE14o- cells (from Dr. Gruenert at University of California San Francisco) were cultured in MEM medium (Gibco) supplemented with 10% FBS (Gibco), 1% L-Glutamine (2mM, Gibco), 1% penicillin (100U/ml, Gibco) and 1% streptomycin (100U/ml, Gibco). Primary human pulmonary alveolar epithelial cells (pHPAEC) were obtained from a lung resection from a patient undergoing pneumectomy for lung cancer. All participants provided written informed consent. Briefly, healthy lung tissue was digested into a single cell suspension using a solution of 0.1% collagenase I/0.25% collagenase II (Worthington Biochemical). Healthy epithelial cells were isolated using fluorescent activated cell sorting (BD FACS Aria III) with an antibody that recognizes CD326, also known as epithelial cell adhesion molecule (EpCAM, clone 1B7, eBioscience) while excluding hematopoietic (CD45, clone 2D1 and CD14, clone 61D3, eBioscience) and endothelial cells (CD31, clone WM59, eBioscience).Following sorting, EpCAM+ primary human pulmonary alveolar epithelial cells (pHPAECs) were cultured for expansion in CnT-Prime Airway epithelial culture medium (CELLnTEC, Berne, CH) supplemented with 1% penicillin (100U/ml, Gibco) and 1% streptomycin (100U/ml, Gibco)1% Pen Strep (Gibco). Immunophenotyping culture-expanded EpCAM+ cells was carried out using flow cytometry (BD FACS Canto LSRII) for the expression of type I and type II epithelial markers podoplanin (clone NZ-1.3 , eBioscience) and CD63 (clone H5C6, eBioscience), respectively. Primary human umbilical vein endothelial cells (pHUVEC, Lonza) were cultured in EBM-2 medium (Lonza) supplemented with 2% FBS and growth factors according to the manufacturers protocols. All cells were maintained at 37°C, 5% CO2 in air. Prior to cell seeding, the microfluidic devices were sterilized by ozone (CoolCLAVE, Genlantis) and the porous membranes were covalently coated with human fibronectin (2.5µg/cm2, Merck-Millipore) or 0.1% gelatin and 2µg/ml collagen I as previously described.[9] Briefly, the membranes were activated by O2-plasma and immediately covered with 5% (3-Aminopropyl)triethoxysilane (Sigma-Aldrich) in H2O. After 20min, the membranes were thoroughly rinsed with deionized

water and covered with 0.1% glutaraldehyde (Sigma-Aldrich). After an additional 20min incubation, the membranes were washed again with deionized water, and then coated with fibronectin and incubated overnight. Prior to cell seeding, the membranes were washed with cell culture medium.

Co-culture experiments: HUVECs (passage 4) were seeded on the basal side of the membrane at $5x10^4$ cells/cm^2, on a 10µm thin membrane with 8µm pores ($6x10^4$ pores/cm^2) After 24h, the lung-on-chip was flipped and epithelial cells were seeded on the apical side of the membrane at $4x10^5$ cells/cm^2. The cells were allowed to adhere and grow for 24h before being stained for fluorescence imaging.

Cell permeability: 16HBE14o- bronchial epithelial cells were used for the cell permeability experiments between passages 2.50 and 2.57. They were seeded at a density of $2.5x10^5$ cells per cm^2 on 10µm thin, porous PDMS membranes (8µm pores, $6x10^4$ pores/cm^2). The cells were allowed to adhere for two hours, followed by replenishing the cell culture medium. The cells were cultured for 72h prior to be used for the permeability assay to ensure confluence. Cell culture medium was replenished daily.

Cell viability and cytokine expression: Cell culture expanded EpCAM+ pHPAECs (passage 3) were used for the cell viability assays as well as for the IL-8 secretion experiments. Cells were seeded on 3.5µm thin PDMS membrane without pores at a density of $4x10^5$ cells/cm^2. The cells were allowed to adhere for 24h before the cell culture medium was replenished. The cells were grown for 48h prior to use. The cell culture medium was changed daily.

Stretching protocol

Once a confluent cell monolayer is formed on the thin membrane, a drop of 50µl of cell culture medium is added on the basal side of the fluidic part. The fluidic part is then flipped with the drop of cell culture medium hanging and mounted onto the pneumatic part. The micro-diaphragm is able to apply a reproducible, three-dimensional cyclic strain to the cells (corresponding to a 10% linear). To cyclically stretch the membrane at a frequency of 0.2Hz, the lung-on-chip is connected to an external electro-pneumatic setup. This setup controls the magnitude of the applied negative pressure as well as the frequency. The pressure-curve is modeled as a sinusoidal wave. The stretch magnitude of 10% linear is within the physiological range of strain, experienced by the alveolar epithelium in the human lung.[10]

Permeability assay

Upon confluence (after 72 hours in culture), the basal compartment was filled with cell culture medium and mounted on the pneumatic part. The cells were either preconditioned by stretch for 19 hours or kept under static conditions for the same amount of time prior to perform the assay. To assess the apical to basal permeability of the epithelial barrier, 1µg/ml FITC-Sodium (Sigma Aldrich) in MEM medium and 1mg/ml RITC-Dextran (70kDa, Sigma-Aldrich) in MEM medium was added from the apical side of the epithelial barrier. The system was allowed to incubate for two hours either under dynamic or static conditions. After two hours of incubation, the fluid gained from the basal side of the barrier was collected and analyzed with a multiwell plate reader (M1000 Infinite, Tecan) at 460nm and 553nm excitation and 515nm and 627nm emission for FITC-Sodium and RITC-Dextran, respectively. The permeability was assessed in terms of relative transport across the epithelial barrier by normalizing the fluorescence intensity signal obtained from the solution sampled in the basal chamber with the fluorescence signal obtained from the standard solution initially added on the apical side of the barrier.

Cell viability and proliferation

To measure cell viability and proliferation, the non-toxic alamar blue (Invitrogen) assay was used according to the manufacturer's protocol. Briefly, the alamar blue reagent was mixed with cell culture medium in a 1:10 ratio. 60µl of the mixture was added to the cell culture well and incubated for one hour at 37°C under static conditions. After incubation, the fluorescence intensity of the cell supernatant was measured using a multiwell plate reader at 570nm excitation and 585nm emission. The amount of fluorescence intensity corresponds directly to the metabolic activity of the cells. The assay was performed at 0h (before applying stretch) and after 24h and 48h of stretching. The same time points were used for the static controls.

IL-8 secretion

IL-8 secretion in the supernatant was measured using an ELISA Kit (R&D Diagnostics) according to the manufacturer's protocol. The supernatant analyzed was collected after 2, 24 and 48 hours of stretching. After collection of supernatant, new media was added. Cells kept under static conditions served as control.

Immunofluorescence imaging

For immunofluorescence imaging, cells were rinsed with PBS and fixed with 4% paraformaldehyde (Sigma-Aldrich) in PBS for 12min at room temperature. After several washing steps with PBS, the cells were permeabilized with 0.2% Triton-X100 (Sigma-Aldrich) in PBS for another 10min. To prevent any unspecific antibody binding, a blocking solution of PBS with 5% FBS and 1% bovine serum albumin (Sigma-Aldrich) was added for 30min. Primary antibodies (E-Cadherin (67A4), Santa Cruz and VE-Cadherin (V1514), Sigma-Aldrich) were diluted 1:100 in blocking solution and incubated for 2h at RT. The corresponding secondary antibodies (Donkey-anti-mouse-AlexaFluor568, Invitrogen and donkey-anti-rabbit-AlexaFluor488, Invitrogen) were diluted 1:200 and Hoechst 33342 (1:10'000, Invitrogen) to counterstain cell nuclei were incubated for 1h at 20°C in dark. After rinsing three times with blocking solution, the specimens were embedded in VectaShield anti-fade medium (Sigma-Aldrich). Images were obtained using a confocal laser scanning microscope (CLSM, Zeiss LSM 710).

Statistics

Data are presented as means ± standard deviation (SD). Differences between two means were determined by two-tailed

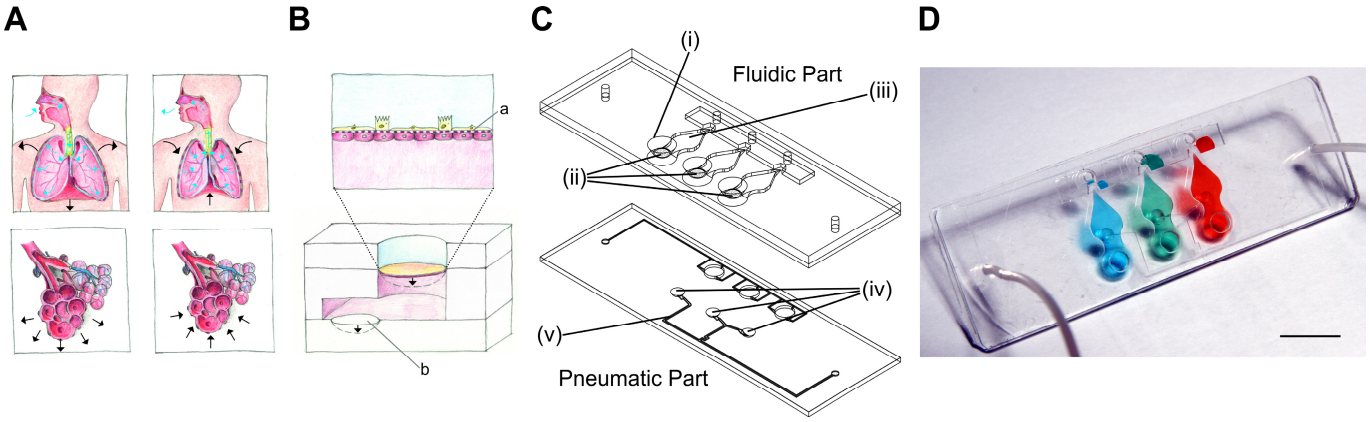

Figure 1. Working-principle and design of the lung-on-chip. A In-vivo, the inspiration is controlled by the diaphragm, whose contraction leads to the three-dimensional expansion of the alveolar sacs. **B** In-vitro, the 3D cyclic mechanical strain of the bioartificial alveolar membrane (a) is provoked by a micro-diaphragm (b) that is actuated by an electro-pneumatic set-up. The bioartificial alveolar membrane consists of a thin, porous and stretchable membrane on which epithelial and endothelial cells are cultured. **C** The lung-on-chips is made of a 25x75mm fluidic and pneumatic part. The fluidic part consists of three alveolar cell culture wells (i) and of thin, porous and flexible membranes (ii), beneath which the basolateral chambers are located (iii). The micro-diaphragms (iv) are integrated in the pneumatic part and connected to pneumatic microchannels (v). **D** Photograph of the lung-on-chip filled with food-dye-colored solutions inside the basolateral chambers. Scale bar: 10 mm.

unpaired Student's T-test and $p<0.05$ was taken as level of significance.

Results and Discussion

Design of the lung-on-chip with the bioinspired respiration mechanism

The air-blood barrier of the lung, with a thickness of about 1 to 2 micrometers,[11] is constantly exposed to a cyclic mechanical stress induced at the organ-level by the diaphragm, the most important muscle of inspiration. It consists of a thin dome shaped sheet of muscle that contracts and thereby increasing the thoracic cavity.[12] The under pressure created by the diaphragm is further transmitted to the complex architecture of the lung, until its most delicate structures, the alveolar sacs (Fig. 1A). Stress concentration is particularly important in the thin alveolar septa that separate adjacent alveoli. This site is constituted by two monolayers of alveolar epithelial cells separated by the basal membrane and the pulmonary microcapillaries.[10] During normal breathing, the respiratory cycle consists of 10 to 12 breathings per minute, with a mechanical strain comprised between 5 to 12% linear elongation.[10] The effects of the mechanical strain have been reported in a number of biological processes, for example in lung development[13,14] or in the evolution of various respiratory diseases, such as acute lung injury,[15] lung fibrosis[16] and other interstitial lung diseases.[17] Although our knowledge about the mechanobiology of the lung, in particular regarding the mechano-responses of lung epithelial cells, has advanced significantly during the last two decades, much remains to be discovered and understood in this research field.[10] This fact is due in large part to the lack of systems able to reproduce the dynamic and structurally complex environment of the alveolar barrier. Indeed, with the exception of the system recently reported by Huh and colleagues,[7] standard systems used to investigate mechanical effects only mimic the respiratory movements, but not the characteristics of the thin alveolar barrier.[10,18] In addition, the experimental conditions of all these systems vary considerably making cross-comparisons between studies difficult. This is particularly true for the applied strain, which is either applied in one direction (cell elongation, e.g. Huh et al.[7]), in two-dimensions (stress of the cell surface area, e.g. Flexcell) or in three dimensions, like it is the case in-vivo and in the present lung-on-chip.

The design of the lung-on-chip presented in this study mimics the alveolar sac environment of the human lung including the mechanical stress induced by the respiration movements (Fig. 1A+B). The bioartificial alveolar barrier consists of a thin, porous and flexible PDMS membrane on which cells are cultured, typically epithelial cells on the apical and endothelial cells on the basal side of the membrane. This barrier is indirectly stretched downwards by the movements of a 40µm thick actuation PDMS membrane that acts as a micro-diaphragm. It is cyclically deflected by a negative pressure applied in a small cavity located beneath the micro-diaphragm. The cavity volume limits the deflection of the micro-diaphragm enabling a clearly defined maximum strain, when the actuation membrane reaches the bottom of the cavity. As the alveolar barrier and the micro-diaphragm are located in a close compartment filled with an incompressible cell culture solution, the pressure applied on the micro-diaphragm is transmitted to the alveolar membrane according to Pascal's law. The maximum three-dimensional mechanical strain applied – set at 10% linear strain – to the alveolar membrane is thus accurately controlled by the volume of the micro-diaphragm cavity.

The reproduction of in-vivo features is a priority to create biologically relevant organs-on-chips. However the ease to use and the robustness of such systems are parameters that are as important in view of their broader use. The design of the present lung-on-chip also addresses those constraints, in particular the precise control of the number of cells seeded in the culturing well, which is a typical and recurrent issue of cell-based microfluidic systems. In such systems, the cells loaded on the chip are not controlled once they enter the microfluidic network,

which often results in an inhomogeneous cellular spatial distribution and the "loss" of cells in the fluidic network outside of the culturing zone. To address this issue, a semi-open design was imagined allowing for an accurate control of the cells seeded on the apical side of the membrane (Fig. 1C-D). Cells are pipetted directly on the thin membrane like in a standard multiwell plate. The problem of the cell seeding on the basal side of the membrane was solved by using an extension of the hanging drop technique (Suppl. Fig.1). Once the cell layer is confluent on the apical side of the membrane, the chip is flipped and a drop of cell culture medium with cells in suspension is added on the basal side of the membrane. After cell adhesion on the basal side of the membrane, the fluidic part of the lung-on-chip is flipped with the cell culture medium drop hanging. The fluidic part is then brought in contact with the lower part of the lung-on-chip and closed. During this step, the drop of cell culture medium is forced into the basal compartment defined between both plates. The excess of solution is pushed outside of the compartment via a microvalve.

The following results demonstrate in a first phase the mechanical functionality and the robustness of the lung-on-chip. In a second phase, the effects of a physiological mechanical strain are demonstrated on lung epithelial cells. The experiments are performed under normal breathing conditions, meaning a breathing cycle of 12 cycles/min, at a physiological level of strain corresponding to 10% linear elongation.

Characterization of the lung-on-chip

Figure 1C illustrates a bioinspired lung-on-chip with three alveolar cell culture wells (i) having each a direct access to a thin, porous and stretchable alveolar membrane (ii). The basal chambers (iii) located under each membrane are filled with dyed solutions confined between the fluidic and the pneumatic parts. The slight over deflection (about 1% linear strain) of the alveolar membrane that results from bringing the two parts together is levelled by a normally closed pneumatic microvalve located between the basal compartment and the over-flow chamber. A slight pressure exerted on the two rubber parts leads to a reversible bonding (Suppl. Fig. 1) that is strong enough to ensure the operation of the chip as well as prevent any leakages. The cyclic mechanical stress of the micro-diaphragm (iv) located in the pneumatic part of the lung-on-chip enables the alveolar barrier to be mechanically stressed at a well-defined level. The home-made electro-pneumatic set-up, connected to the microchannels of the pneumatic part (v), generates a negative pressure with a sinusoidal function that reproduces the respiration parameters during normal breathing. The maximum strain in the alveolar membrane is evaluated by comparing two pictures taken in the center of the alveolar membrane at rest and when the micro-diaphragm is completely deflected (Suppl. Fig. 2). At maximum deflection, the strain in the alveolar membrane accounts for a maximal linear elongation of 10%.

The microstructuring-lamination process developed to fabricate the thin, porous and flexible membrane produces reliable and reproducible features. The membranes can be produced with thicknesses of either 3.5 or 10µm, and with pore sizes and densities of either 3µm with 800'000pores/cm^2 or 8µm with 60'000pores/cm^2 with little variations in pore densities (Fig. 2A). The pore sizes and densities of the produced PDMS membrane correspond to those of commercially available cell culture inserts.

Reconstitution of the lung alveolar barrier

The integrity of the lung alveolar barrier is one of the most critical parameters of a healthy lung. If damaged it leads to fluid infiltration in the alveolar sacs that may cause lung edema and other types of pulmonary diseases. The integrity of the barrier is guaranteed by a number of proteins forming either tight junctions or adherens junctions. Tight junction proteins are responsible for the formation of functional epithelial and endothelial barriers, and primarily function as diffusion barrier.[19] Adherens junctions link actin filaments between neighboring cells, maintain tissue integrity and translate mechanical forces throughout a tissue via the cytoskeleton.[20]

To recapitulate a functional epithelial barrier, a co-culture of bronchial epithelial cells (16HBE14o-) and primary endothelial cells (HUVEC) were cultured on a 10µm thin, porous membrane coated with fibronectin (Fig. 2D). HUVECs and 16HBE14o-

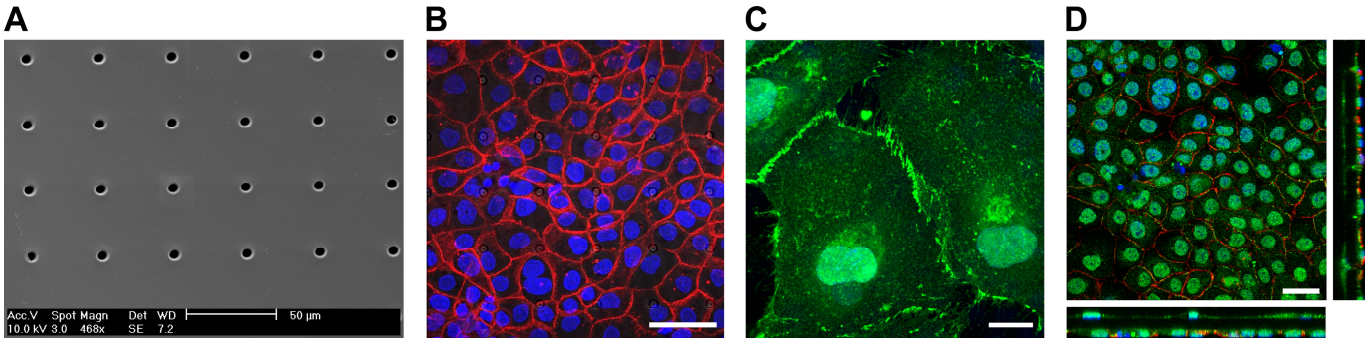

Figure 2. Porous and flexible PDMS membrane used as cell culture substrate. **A** SEM image of a PDMS membrane with 8µm pores. **B** Z-projection of a confluent layer of lung epithelial cells (16HBE14o-) stained for adherens junctions E-cadherin (red) and for cell nuclei (blue). The pores of the porous membrane can be seen in the background. **C** Immunofluorescence image of endothelial cells (HUVEC) stained for adherens junction VE-Cadherin (green) and for cell nuclei (blue). **D** Confocal picture of 16HBE14o- and (HUVEC) co-culture, stained for E-Cadherin (red), VE-cadherin (green) and cell nuclei (blue). Cell-cell contacts between the epithelial and the endothelial cells can be seen through the pores (white arrows). Scale bars: 50, 50, 20 and 30µm.

bronchial epithelial cells were seeded on the basal side and on the apical side of the membrane, respectively. The epithelial and endothelial layers grew to confluence in two to four days building a homogeneous and tight barrier. Tight junction proteins (e.g. zona-occludens-1 (Z0-1)) and adherens junction proteins (e.g. E-cadherin) accumulated at the cellular interface of the epithelial layer forming strong cell-cell contacts (Fig. 2B). On the endothelial side, vascular endothelial cadherin (VE-cadherin) based adherens junction expression was also attested confirming the formation of a tight endothelial barrier. The brush borders of the endothelial cells are typical to endothelial layers (Fig. 2C). Cell-cell contacts between the endothelial and the epithelial layer could also be confirmed through the 8µm pores (Fig. 2D).

Influence of the mechanical stress on the barrier permeability

The alveolar epithelial barrier with its huge surface in contact with air makes it one of the most important ports of entry in the human body. The alveolar barrier is constantly exposed to a variety of xenobiotics that are either cleared by the epithelium or taken up by the air-blood barrier. A portion of these molecules enter in the blood stream and are transported in other organs, which they may affect. Although it was shown in different in-vivo studies that the mechanical strain highly affects the uptake of such molecules,[21] only little is known about the exact transport mechanisms taking place.[22] The role of the respiratory movements, in particular the dynamics taking place in the tight junctions, is unknown and requires the advent of novel devices enabling such investigations.[19]

The lung-on-chip with a monolayer of bronchial epithelial cells was used to investigate the effects of the physiological strain (10% linear) on the transport of specific molecules across the epithelial barrier. A monolayer of bronchial epithelial cells (16HBE14o-) was cultured on a fibronectin coated porous PDMS membrane (8µm pores). 16HBE14o- cells have similar permeability properties than primary human alveolar epithelial cells,[23] which makes them a good model for permeability studies. Furthermore, a monoculture of epithelial cells was used to model the transport within the lung, because endothelial cells have a much higher permeability[24] and were therefore neglected in this model. The permeability assays were performed, either in static or in dynamic mode, with two different molecules dispensed simultaneously to the epithelial layer. The effect of the physiological strain was assessed on the transport of hydrophilic molecules (using FITC-sodium) and in regards to the epithelial barrier integrity (RITC-Dextran). The experiments reveal that the permeability of small hydrophilic molecules is significantly ($p<0.005$) increased if the cells are kept in a dynamic (n=3) compared to a static environment (n=6) (Fig. 3). The relative increase in transport is about 46% (5.68±0.52% vs. 3.88±0.47%). This increase cannot be explained by the increase in diffusive transport due to the stretching of the pores. In fact, the diffusive transport scales linearly with the pores surface area, which is 21% in the present case. In addition, the pores array is covered by a confluent layer of cells.On the other hand, the physiological strain did not affect the cell layer integrity, since no significant

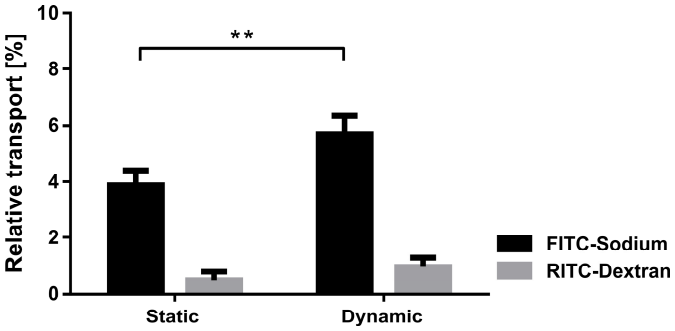

Figure 3. The effect of cyclic strain on the permeability of lung epithelial 16HBE14o- cells. The relative transport of a small molecule (FITC-sodium) across the monolayer significantly increased upon a physiologic cyclic strain whereas the barrier integrity was not affected by the strain (no significant transport increase for RITC-Dextran). Cyclic stretch was applied for 21 hours (dynamic n=3) and a control was kept in static conditions (static n=6) (mean values ± SD, $p<0.005$).

increase of the permeability was observed for RITC-Dextran. This finding is supported by immunofluorescence images of the 16HBE14o- cells, which did not show any significant differences in morphology nor in tight junctions comparing the static and dynamic condition (Suppl. Fig. 3).

This experiment showed that the epithelial barrier permeability is significantly affected by the physiological strain produced in the lung-on-chip. These results are in good agreement with the increased permeability reported for hydrophilic solutes in an in-vivo study upon distention in human lungs.[25] The transport mechanism which takes place is not fully understood. The most accepted theory is that due to the stretching of the cells, the intercellular junction pores are also stretched, which then leads to an enhanced permeability for hydrophilic molecules.[26] These results illustrate the importance to investigate the effects of the breathing motions on the epithelial barrier permeability. Such issues are of prime relevance for toxicology questions, as well as for inhalable formulations that are expected to be developed in a near future.[27,28]

Influence of the mechanical stress on the activity of primary human pulmonary alveolar epithelial cells

Primary human pulmonary alveolar epithelial cells were selected using the common epithelial marker EpCAM (CD326). Following sorting, culture-expanded EpCAM+ cells demonstrated a cuboidal morphology and expression of markers typically found on type I and type II alveolar epithelial cells of the lower airway (Fig. 4A,C). Expanded EpCAM+ pHPAECs were then cultured on thin, porous and flexible membranes. The cells reached confluence after 24h (Figure 4B). Further, the cells could be cultured for up to 21 days on the membranes.

To determine the influence of the strain on the metabolic activity of the pHPAECs, alamar blue assay was performed with static cells and cells before and after being stretched (Fig. 5A). Alamar blue measures the reductive potential of the cells and is a measure for both, cell proliferation and cell viability. The fluorescence intensity of the cells under static condition almost doubled in the first 24h, suggesting that the cells are still proliferating (5239.5 ± 685.6 vs. 9391.7±1513.3 a.u., n=6).

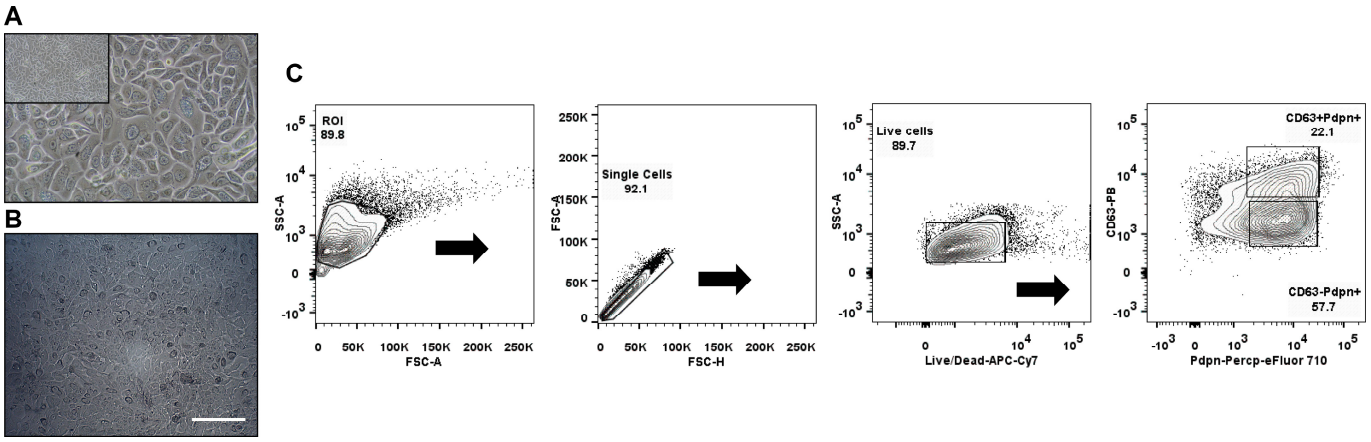

Figure 4. Primary human pulmonary alveolar epithelial cells. A Representative phase contrast image of culture expanded EpCAM+ pHPAECs. **B** Phase-contrast picture of a confluent monolayer of EpCAM+ pHPAECs cultured on the alveolar membrane (Scale bar 200µm). **C** Flow cytometric density plots showing expression of both type I (Pdpn-Percp-eFluor 710) and type II (CD63-PB) surface markers on culture-expanded EpCAM+ cells. Pdpn, podoplanin; PB, Pacific Blue; ROI, region of interest

Similarly, the cells that were grown under static conditions followed by 24h of stretch almost doubled their fluorescence intensity (5569.7±655.6 vs. 10728.7±1147.3 a.u., n=6). Therefore, 10% linear cyclic stretch does not interfere with the proliferation of pHPAECs. Furthermore, cyclic stretch at this magnitude does not increase cell injury or cell death in primary human pulmonary alveolar epithelial cells. However, if the cells are stretched for 48h the metabolic activity is significantly higher compared to the static control (9860.2±471 vs. 8164.8±831.4 a.u., n=6).

These findings are supported by the study of McAdams et al., in which they exposed human alveolar-like adenocarcinomic cell line A549 to 16% linear strain.[29] Similarly to our findings, they did not observe any significant difference between cells stretched for 24h and cells cultured in static conditions. However, after 48h of stretch, the proliferation of stretched cells was significantly enhanced.[29] They also showed that cyclic strain with a magnitude of 16% linear elongation did not change the percentage of dead cells compared to a non-stretched control over 48h. In contrast, several studies with primary rat ATII cells show a significant increase in apoptosis and cell death even at linear stretch as low as 6%.[30,31] However, with our primary human pulmonary alveolar cells we could not observe such a behavior. It is not known, whether these differences in effect of stretch on cell proliferation and viability is due to interspecies differences or not.

The supernatant from pHPAEC cells under static and dynamic condition was further sampled at different time points and analyzed for their cytokine release patterns. Interleukin-8 (IL-8), a pro-inflammatory cytokine known to be upregulated in cell lines upon mechanical stretch,[32,33] was measured by ELISA (Fig. 5B). After 2h of stretching, no difference between dynamic and static conditions was observed (0.71±0.08 ng/ml vs. 0.58±0.15 ng/ml, n=3). After 24h of stretch, a tendency of a higher IL-8 secretion was seen compared to static control (10.97±2.8ng/ml vs. 6.54±4.64ng/ml, n=3). However, after 48h of stretch, the IL-

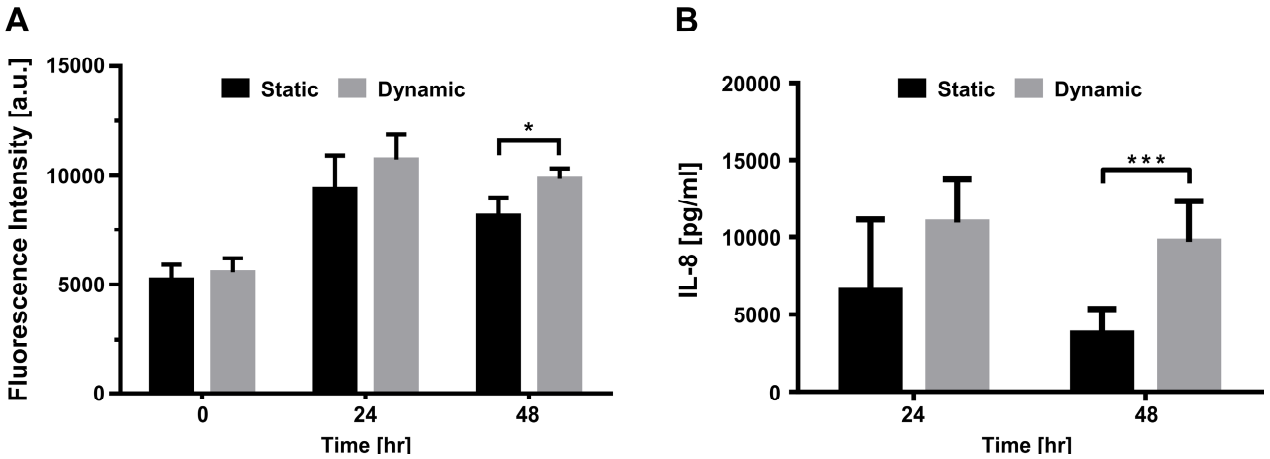

Figure 5. The effect of cyclic strain on the activity of primary human pulmonary alveolar epithelial cells. A The fluorescence intensity of alamar blue increases similarly in the first 24h in both conditions, static and stretched (dynamic), showing, that proliferation of primary alveolar epithelial cells is not affected by cyclic stretch. However, after 48h of stretch the metabolic activity is significantly higher in the stretched cells than in the static control. (n=6, mean values ± SD, * p<0.05) **B** The IL-8 secretion of primary alveolar cells being stretched (dynamic) compared to a static control (static). After 24 hours of cyclic strain there is a tendency to an increased secretion of IL-8. After 48 hours the secretion of IL-8 is significantly higher compared to the static control (n=3), mean values ± SD, p<0.001.

8 concentration found in the supernatant of the stretched cells was 2.5x higher than the IL-8 concentration in the static control (9.7±2.65 ng/ml vs. 3.81±1.55 ng/ml). The knowledge of the effect of stretch on IL-8 production in the lung is controversial and restricted to A549 cells only. Two studies showed that IL-8 secretion is increased in A549 already after 5min to 4h with low linear stretch of 2% and 5%, respectively.[34,35] In contrast, several studies could not see this increase in IL-8 production in A549 cells in the first few hours even with stretch magnitude of 10%.[36,37] In our study, we could not observe an increase after 2h in primary human pulmonary alveolar cells, either. Jafari et al. only found a higher IL-8 production when stretching the cells with a linear elongation of 15%.[36] Ning & Wang further show a stretch magnitude dependent IL-8 secretion, which does not depend on the stretch frequency.[35] The only study looking at longer periods of stretch (up to 48h) could observe an increase of IL-8 production in A549 when stretched at 30% linear stretch, but not when stretched at 20% linear stretch.[33] To our knowledge, our study shows for the first time that over longer periods of stretch, IL-8 secretion is enhanced in primary human pulmonary alveolar epithelial cells.

Conclusion

To better model the in-vivo conditions of the biophysical and cellular microenvironment, new and more accurate in-vitro models are needed. Unlike standard cell cultures, organs-on-chip are widely seen as promising candidates capable to predict the human responses to drugs.

This bioinspired lung-on-chip mimics the microenvironment of the lung parenchyma by reproducing the thin alveolar barrier constantly exposed to the respiratory movements. A flexible, thin and porous membrane, on which a co-culture of epithelial and endothelial cells are cultured, is cyclically deflected by a micro-diaphragm, whose function is similar to that of the in-vivo diaphragm. The effects of the breathing movements were investigated using a bronchial epithelial cell line as well as primary human lung epithelial cells from patients. With this device we could demonstrate that the mechanical stress profoundly and significantly affect the epithelial barrier permeability. In addition, the metabolic activity of primary human pulmonary alveolar epithelial cells cultured in dynamic mode was found to be significantly higher than cells cultured in static mode. Similarly, a significantly higher production of the inflammation marker IL-8 was found in these cells. To the best of our knowledge, this is the first time that the effects of mechanical strain on human healthy primary cells derived from patients have been investigated.

Although, the main challenge of organs-on-chip systems is to best reproduce the in-vivo conditions, a second challenge is to make such device as robust and reproducible as possible. This aspect is central in view of a wider acceptance of those systems by cell biologists, toxicologists and pharmacologists. The strategy followed during the development of the present device was therefore aimed at designing a system that would combine the ease to handle (e.g. compatible with multi-pipette), the reproducible control of the cultured conditions (number of cells cultured on the membrane and defined level of mechanical strain) and the recapitulation of the main in-vivo features. Such systems are widely expected to better predict the human responses to drugs, and present a great possibility to improve the selection of drug candidates early in the drug discovery process.

Acknowledgements

The authors are very grateful to the Gebert-Rüf Stiftung (GRS-066/11), to the Swiss Commission for the Technology and Innovation (CTI 15794.1 PFLS-LS), the Swiss National Science Foundation (315230_141127) and the Lungenliga Bern for their generous financial support. They also would like to thank Prof. Dr. Robert Rieben (University of Berne) for generously providing primary human umbilical vein endothelial cells (pHUVEC). We thank Dr. Marco Alves and Aline Schoegler for providing advice and materials for ELISA. We also acknowledge the Flow Cytometry Core of the Department of Clinical Research of the University of Berne. Images were acquired on equipment supported by the Microscopy Imaging Center of the University of Berne. A patent on the microfluidic device described is pending.

References

1. F. Pammolli, L. Magazzini, and M. Riccaboni, *Nat. Rev. Drug Discov.*, 2011, **10**, 428–38.
2. H. Olson, G. Betton, D. Robinson, K. Thomas, a Monro, G. Kolaja, P. Lilly, J. Sanders, G. Sipes, W. Bracken, M. Dorato, K. Van Deun, P. Smith, B. Berger, and a Heller, *Regul. Toxicol. Pharmacol.*, 2000, **32**, 56–67.
3. J. H. Sung, M. B. Esch, J. Prot, C. J. Long, A. Smith, J. J. Hickman, and M. L. Shuler, *Lab Chip*, 2013, **13**, 1201–12.
4. Y. Zheng, H. Fujioka, S. Bian, Y. Torisawa, D. Huh, S. Takayama, and J. B. Grotberg, *Phys. Fluids (1994).*, 2009, **21**, 71903.
5. N. J. Douville, P. Zamankhan, Y.-C. Tung, R. Li, B. L. Vaughan, C.-F. Tai, J. White, P. J. Christensen, J. B. Grotberg, and S. Takayama, *Lab Chip*, 2011, **11**, 609–19.
6. D. Huh, H. Fujioka, Y.-C. Tung, N. Futai, R. Paine, J. B. Grotberg, and S. Takayama, *Proc Natl Acad Sci USA*, 2007, **104**, 18886–91.
7. D. Huh, B. D. Matthews, A. Mammoto, M. Montoya-Zavala, H. Y. Hsin, and D. E. Ingber, *Science (80-.).*, 2010, **328**, 1662–1668.
8. J. C. McDonald and G. M. Whitesides, *Acc. Chem. Res.*, 2002, **35**, 491–9.
9. C. P. Ng and M. A. Swartz, *Am. J. Physiol. Heart Circ. Physiol.*, 2003, **284**, H1771–7.
10. C. M. Waters, E. Roan, and D. Navajas, *Compr. Physiol.*, 2012, **2**, 1–29.
11. P. Gehr, M. Bachofen, and E. R. Weibel, *Respir. Physiol.*, 1978, **32**, 121–40.
12. J. B. West, *Adv. Physiol. Educ.*, 2008, **32**, 177–84.
13. V. D. Varner and C. M. Nelson, *Development*, 2014, **141**, 2750–2759.
14. T. Mammoto, A. Mammoto, and D. E. Ingber, *Annu. Rev. Cell Dev. Biol.*, 2013, **29**, 27–61.

15. M. Plataki and R. D. Hubmayr, *Expert Rev. Respir. Med.*, 2010, **4**, 373–85.
16. M. E. Blaauboer, T. H. Smit, R. Hanemaaijer, R. Stoop, and V. Everts, *Biochem. Biophys. Res. Commun.*, 2011, **404**, 23–7.
17. B. Suki, D. Stamenović, and R. Hubmayr, *Compr. Physiol.*, 2011, **1**, 1317–51.
18. D. J. Tschumperlin and J. M. Drazen, *Annu. Rev. Physiol.*, 2006, **68**, 563–83.
19. E. Steed, M. S. Balda, and K. Matter, *Trends Cell Biol.*, 2010, **20**, 142–9.
20. C. M. Niessen, D. Leckband, and A. S. Yap, *Physiol. Rev.*, 2011, **91**, 691–731.
21. G. Taylor, *Adv. Drug Deliv. Rev.*, 1990, **5**, 37–61.
22. H. Smyth and A. Hickey, *Controlled Pulmonary Drug Delivery*, 2011.
23. B. Forbes and C. Ehrhardt, *Eur. J. Pharm. Biopharm.*, 2005, **60**, 193–205.
24. S. Braude, K. B. Nolop, J. M. Hughes, P. J. Barnes, and D. Royston, *Am. Rev. Respir. Dis.*, 1986, **133**, 1002–1005.
25. J. D. Marks, J. M. Luce, N. M. Lazar, J. N. Wu, A. Lipavsky, and J. F. Murray, *J. Appl. Physiol.*, 1985, **59**, 1242–8.
26. J. M. B. Hughes, 2001, **236**, 231–236.
27. M. Haghi, H. X. Ong, D. Traini, and P. Young, *Pharmacol. Ther.*, 2014.
28. Z. Liang, R. Ni, J. Zhou, and S. Mao, *Drug Discov. Today*, 2014, **00**, 1–10.
29. R. M. McAdams, S. B. Mustafa, J. S. Shenberger, P. S. Dixon, B. M. Henson, and R. J. DiGeronimo, *Am. J. Physiol. Lung Cell. Mol. Physiol.*, 2006, **291**, L166–74.
30. D. Tschumperlin and S. Margulies, *Am. J. Physiol. Lung Cell. Mol. Physiol.*, 1998, **275**, L1173–83.
31. S. P. Arold, E. Bartolák-Suki, and B. Suki, *Am. J. Physiol. Lung Cell. Mol. Physiol.*, 2009, **296**, L574–81.
32. D. Quinn, *CHEST J.*, 1999, **116**, 89S.
33. N. E. Vlahakis, M. a Schroeder, a H. Limper, and R. D. Hubmayr, *Am. J. Physiol.*, 1999, **277**, L167–73.
34. L.-F. Li, B. Ouyang, G. Choukroun, R. Matyal, M. Mascarenhas, B. Jafari, J. V Bonventre, T. Force, and D. a Quinn, *Am. J. Physiol. Lung Cell. Mol. Physiol.*, 2003, **285**, L464–75.
35. Q. Ning and X. Wang, *Respiration*, 2007, **74**, 579–85.
36. B. Jafari, B. Ouyang, L.-F. Li, C. a Hales, and D. a Quinn, *Respirology*, 2004, **9**, 43–53.
37. A. Tsuda, B. K. Stringer, S. M. Mijailovich, R. a Rogers, K. Hamada, and M. L. Gray, *Am. J. Respir. Cell Mol. Biol.*, 1999, **21**, 455–62.